

DESIGN OF A BODY FREEDOM FLUTTER FLIGHT MODEL WITH CONVENTIONAL CONFIGURATION

Xinhai Tian^{1,2}, Yingsong Gu^{1,2*}, Zhichun Yang^{1,2}

School of Aeronautics, Northwestern Polytechnical University, Youyi Road 127, Xian 710072, P.R. China National Key Laboratory of Strength and Structrual Integrity, Xian 710065, P.R. China * guyingsong@nwpu.edu.cn

Abstract

When the short-period modal frequency of an aircraft is close to the elastic modal frequency of a flexible wing structure, it is prone to cause rigid-elastic coupling, leading to a special kind of flutter - body freedom flutter. Body freedom flutter is commonly found in large aspect ratio tailless or forward-swept wing configuration, and this paper investigates the design of a body freedom flutter flight model for conventional configuration with short fuselage. For the designed configuration, the influences of the wing swept angle and inertia parameters (with varied mass and position of the payload) on its flutter characteristics (flutter speed and flutter frequency) are analyzed. The calculation results show that the sweptback wing layout is more prone to body freedom flutter than the straight wing configuration, and the flutter speed and flutter frequency decrease with the increase of the wing swept angle. When the swept angle is large enough, the flight model will exhibit body freedom flutter. The flutter speed is decreasing as the mass of payload increasing. Interestingly, the futter speed first decreases and then increases as the mass center of the payload moving forwardly, and the flutter frequency monotonically keeps increasing when the gravity center of the whole model is forward. Correspondingly, the coupling between the pitch mode and the bending mode gets stronger. However, the flutter phenomenon disappears when the mass of payload is moved forward to a certain position. A prototype vehicle has been built and the theoretical model is validated against the modal test results. This study provides a new perspective in understanding the body freedom flutter phenomenon for air vehicles of conventional configuration.

Keywords: body freedom flutter; conventional configuration; flight model; wing swept angle; inertial parameters

1. Introduction

When the short-period modal frequency of an aircraft is close to the elastic modal frequency of a flexible wing structure, it is prone to cause rigid-elastic coupling, leading to a special kind of flutter-body freedom flutter (BFF). The physical mechanism beneath the BFF phenomenon has been revealed for a long time [1]-[3]: an aeroelastic instability dominated by the coupling between wing bending and the short period modes.

So far, most of the research work on BFF is directed towards blended wing body (BWB) configuration. Several past studies have examined the effect of various structural and physical parameters on the flutter characteristics of wings, including mass, mass moment of inertia, elastic and torsional modulus, etc. [4]. The effects of inertial and constitutive properties on BFF for flying wings have also been investigated. For example, an increase in fuselage mass leads to a significant reduction in the flutter speed. However, different center of gravity locations of the fuselage can lead to different flutter modes, as the pitch inertia of the fuselage can have a significant effect on the frequency of the short-period modal [5].

As for the BFF test of the flying wing model, the author's group has also carried out some explorations. The influence of support stiffness on the nature mode and BFF characteristics were investigated [6]. It is indicated that one may obtain similar BFF result to the free-free case by carefully adjusting the

combination of the support stiffness of the vertical spring and torsional spring to ensure the pitching mode frequency exceeding the plunging mode frequency by a certain extent. Moreover, A novel quasi-free flying suspension system capable of releasing pitch, plunge and yaw degrees of freedom is designed and implemented in the wind tunnel flutter test [7]. The influence of the mass balance at the nose on the flutter results is also explored [8].

Recently, researchers have again used a flying wing model for wind tunnel tests to investigate the effects of wing sweep angle, mass of tip weights, and location of weights along the wingspan on the flutter speed and frequency of BFF. The results show that a higher sweep angle leads to increased sensitivity of flutter speeds to changes in mass of tip weights or changes to spanwise location of the weights [9].

In recent years, with the emerging unconventional aircraft designs, there are still needs in characterizing the potential BFF phenomenon in conventional configurations but with very short fuselage like General Dynamics RB-57F [10]. Motivated by this issue, we have designed and built a scaled BFF vehicle of this kind for flight flutter testing study. Currently, the ground vibration test (GVT) and model updating have already been finished, and the taxiing and preliminary flight were conducted.

In this study, for the finite element model of designed configuration, the influences of the wing sweep angle and inertia parameters (with varied mass and position of the payload) on its flutter characteristics (flutter speed and flutter frequency) are analyzed firstly. Then, A prototype vehicle has been built and the theoretical model is validated against the GVT results. Finally, Lessons learned are summarized and pertinent conclusions are drawn.

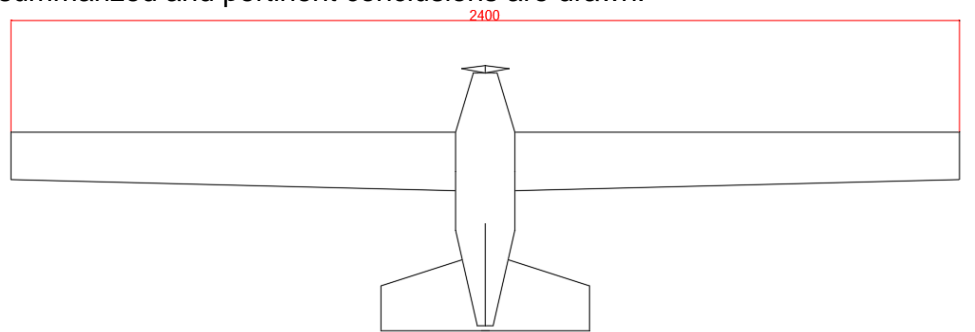


Figure 1 – Aerodynamic layout with straight wing.

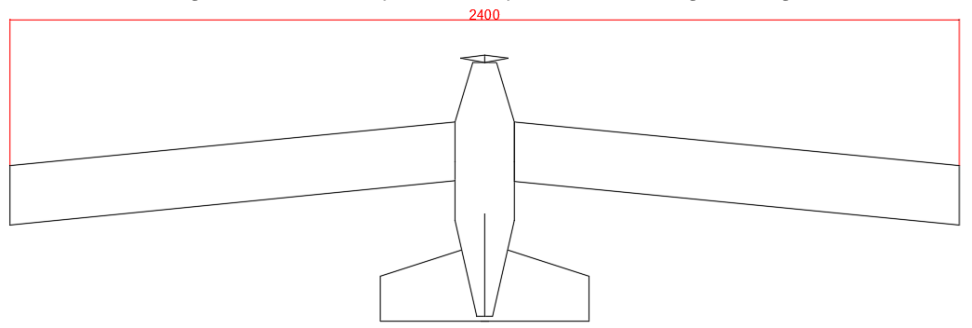


Figure 2 – Aerodynamic layout with swept wing.

2. Design of BFF Vehicle with conventional configuration

In this section, design for the aerodynamic and structure layout is introduced herein for the two conventional configuration BFF vehicles.

2.1 Aerodynamic design

To "produce" BFF in a conventional configuration vehicle, the fuselage should be as short as possible, which will result in a lowest pitch inertia. For this purpose, two different aerodynamic layouts have been considered, a straight wing and swept wing layout as shown in Figure 1 and Figure 2 respectively. Both have a wing span of 2.4m and a root shoot ratio of 1. Moreover, we considered three kinds of swept angles, which are 5.7 deg, 11.3 deg and 16.7 deg, respectively. A comparison of some

parameters of the two layouts is shown in Table 1.

Table 1 – A comparison of some parameters of the two aerodynamic layouts.

Parameter	straight wing	swept wing
Wing span/m	2.4	2.4
Wing area/m ²	0.324	0.36
Swept angle/°	0	11
Chord length/m	0.135	0.15
Fuselage length/m	0.64	0.64
Fuselage width/m	0.15	0.15

2.2 Structural design

The main support structure inside the fuselage is two aluminum beams with sufficient stiffness, located at the lower front and upper rear of the fuselage, as shown in Figure 3(a). The wing is designed with flexible structure made of aluminum spar covered by foam and fastened to the fuselage using a cross-beam structure, as shown in Figures 3(b), 3(c), and 3(d). The tails are attached directly to the fuselage using a length of carbon fiber tubing, which is covered with foam to maintain the shape, as shown in Figure 3(e). The final structural shapes of the two layouts are shown in Figures 4 and 5 respectively.

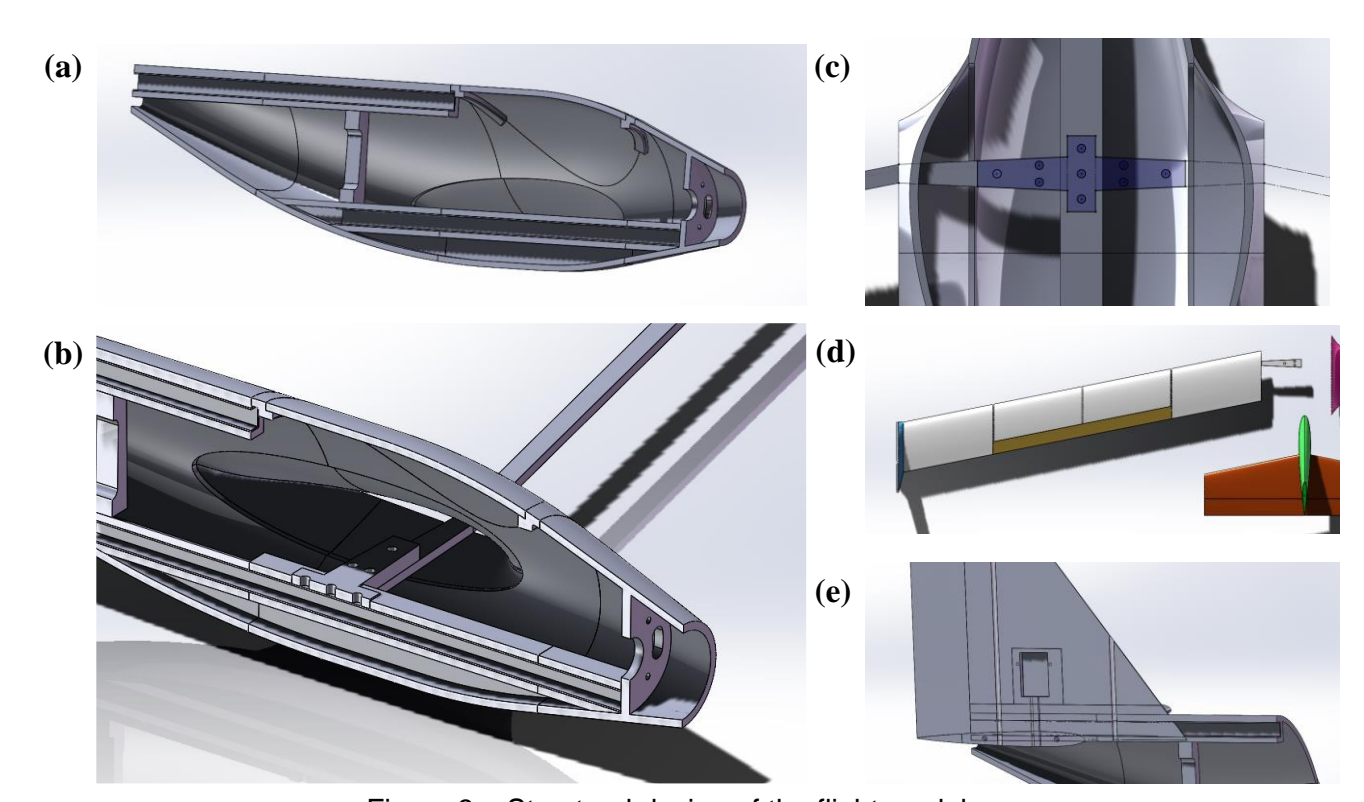


Figure 3 – Structural design of the flight model

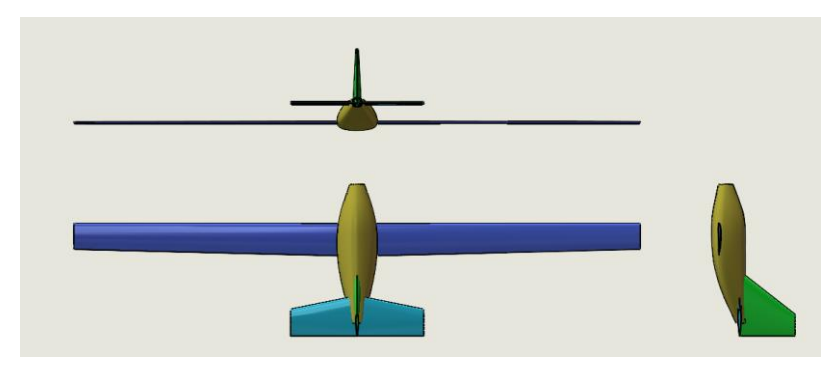


Figure 4 – Structural layout for the BFF vehicle with straight wing

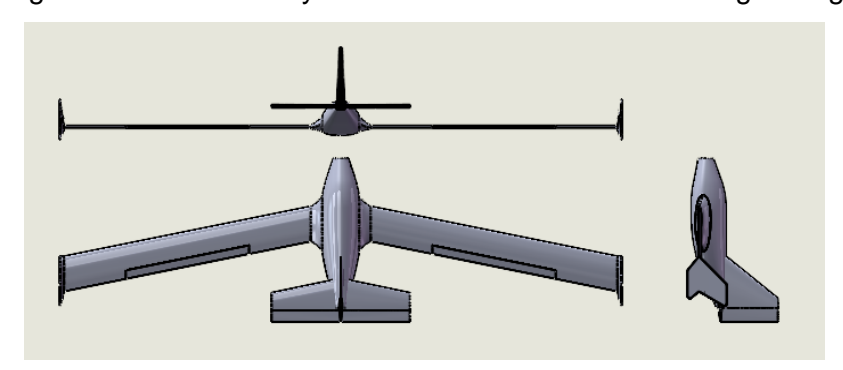


Figure 5 – Structural layout for the BFF vehicle with swept wing

3. Structural dynamic modeling and flutter analysis

In this section, structural dynamic modeling is established for the two structural layouts and flutter analysis are carried out with varied mass and position of the payload.

3.1 Structural dynamics

According to the CAD layout of the BFF vehicle, the FEM is built as show in Figure 6. Only the FEM with a swept angle of 11.7 deg is given here, because the models with different structural layouts differ only in the wing swept angle, and they all have the same fuselage and mass distribution.

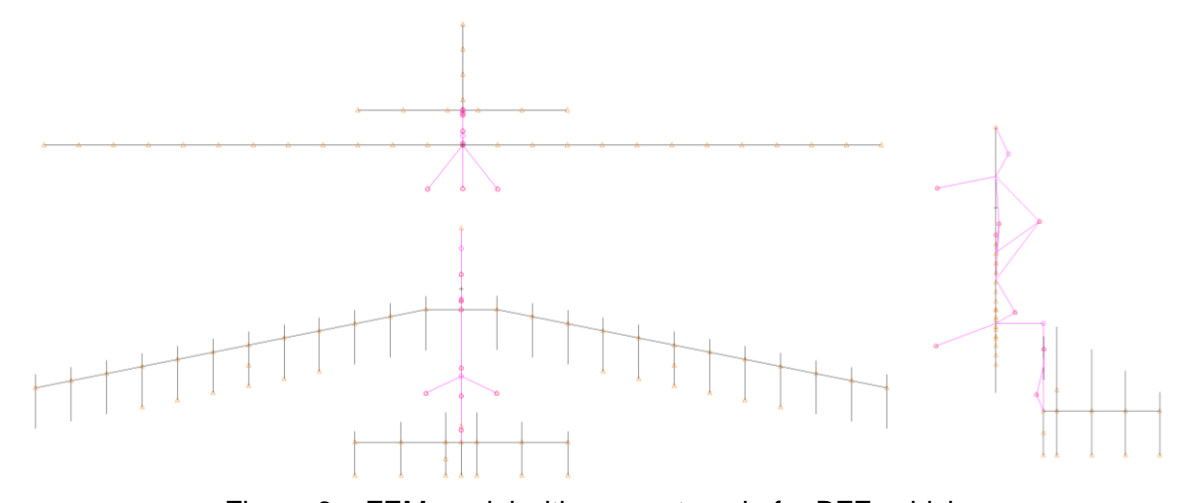


Figure 6 – FEM model with a swept angle for BFF vehicle

The beam elements are applied to model the elastic wing spar, and concentrated mass elements are adopted for inertial distribution modeling of the vehicle according to the CAD layout. Fuselage and empennage structures are considered as rigid beam. All the control surfaces are simplified as concentrated mass elements.

The total weight of the flight model is 3.5kg, including landing gear, battery and control system etc. The normal modal analysis results for different configurations are listed in Table 2. In the next section, flutter analysis is carried out for different configurations.

Table 2 – Modal frequency comparison (unit: Hz).

Madaa	Wing swept angle/deg			
Modes	0.0	5.7	11.3	16.7
1 st sym wing bending	2.98	2.80	2.79	2.92
1 st anti sym wing bending	11.13	11.22	10.97	10.59
2 nd sym wing bending	17.38	17.11	16.63	15.99
2 nd anti sym wing bending	18.58	17.97	17.68	16.84

3.2 Flutter analysis

3.2.1 Straight wing

The straight wing configuration is analyzed firstly. Consider a payload mass of 0.4kg at different locations in the fuselage, which will result in different inertia moments. The DLM model is built for the lifting surfaces as shown in Figure 7. The wing tip device and vertical tail surface are not considered here because only symmetric flutter is interested. Flutter analysis is carried out using incompressible aerodynamics by Nastran. The V-G diagrams under different payload locations are shown in Figure 8.

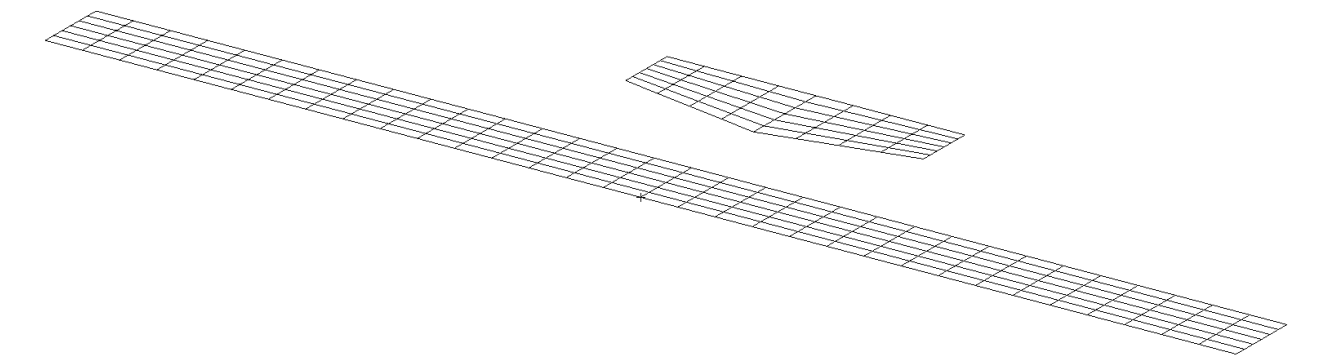


Figure 7 – DLM lifting surface model of the straight wing layout.

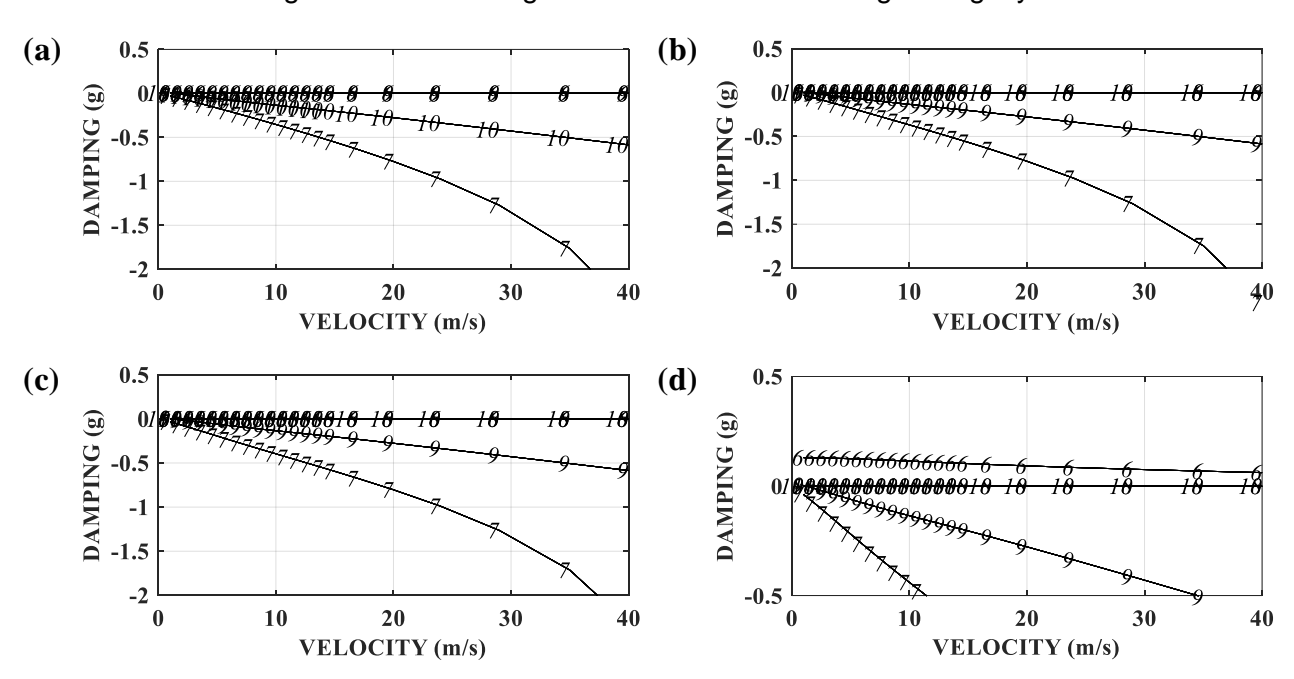


Figure 8 – The V-G diagrams with the payload located (a) 0.33m, (b) 0.25m, (c) 0.20m, (d) 0.15m behind the cross-beam of the fuselage.

Observably, for straight wing configuration with defined size, no flutter occurs at any location of the payload within the analyzed range. Moreover, the payload location is too far forward, which will cause the flight model to be unbalanced in the 6th order mode. That is, the straight wing layout is less prone to BFF.

3.2.2 Sweptback wing

Flutter analysis was first performed for different swept angle layouts with the same 0.4kg payload, which is located 0.15m behind the cross-beam of the fuselage. The DLM model is built for the lifting surfaces as shown in Figure 7. Again, only the case with a swept angle of 11.3 deg is given here. The V-G and V-F diagrams under different swept angle are shown in Figure 10. The flutter speeds and flutter frequencies at different swept angles are listed in Table 3.

It can be seen that the inability of aircraft is eliminated when the swept angle is 5.7 deg and that the 7th order damping is about to go through zero at around 50m/s. Due to flight speed limitations, we require the model to have the lowest possible flutter speed. When the swept angle is increased to 11.3 deg, it is found that the critical flutter point is corresponding to a typical BFF dominated by the

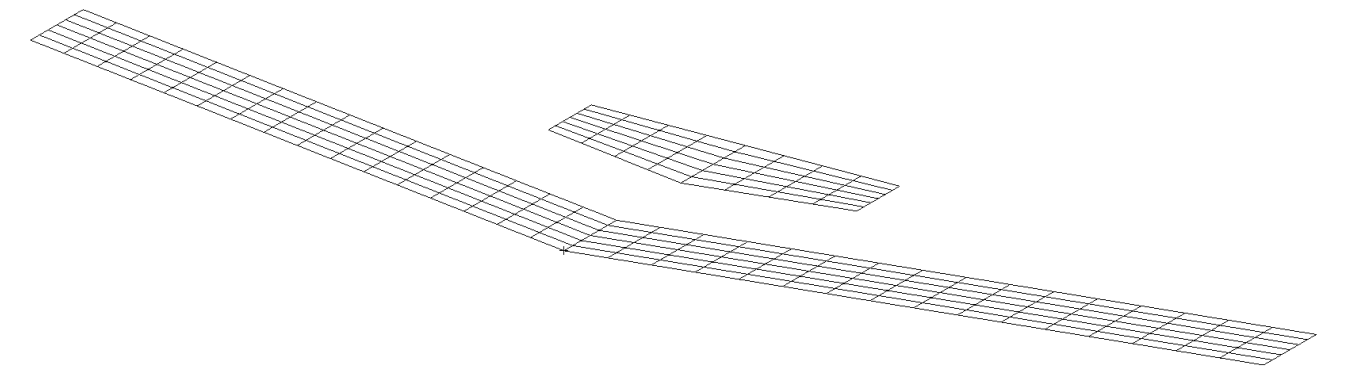


Figure 9 – DLM lifting surface model of the sweptback wing layout with swept angle of 11.3 deg.

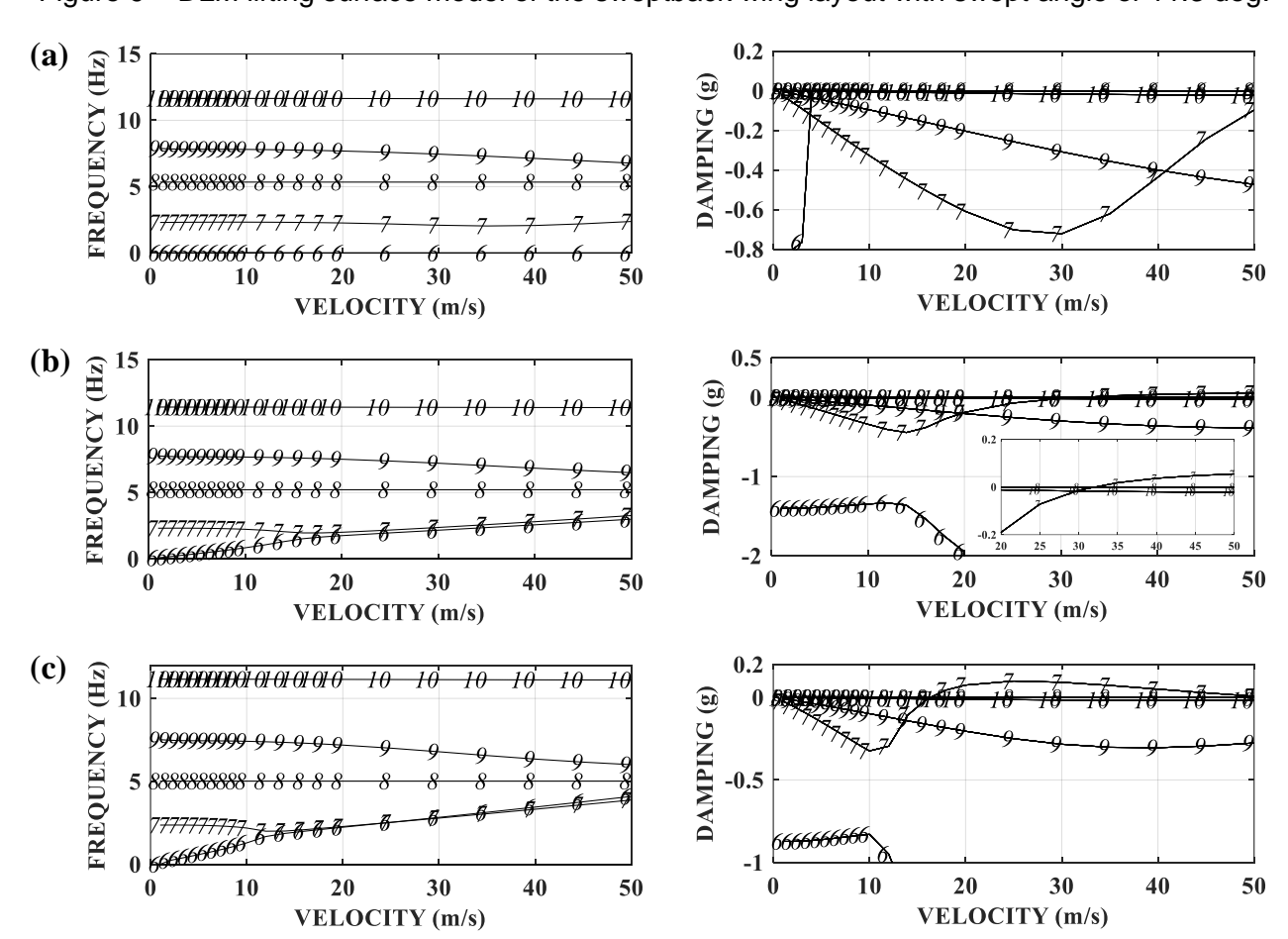


Figure 10 – The V-G diagrams with a swept angle of (a) 5.7 deg, (b) 11.3 deg and (c) 16.7 deg.

Table 3 – The flutter speeds and flutter frequencies with different swept angles.

Swept angle / deg	Flutter speed / m/s	Flutter frequency / Hz
5.7	/	/
11.3	32.1	2.45
16.7	16.3	2.10

pitching mode and wing 1st symmetric bending mode, with a flutter speed of 32.1 m/s and flutter frequency of 2.45 Hz. When the swept angle is increased to 16.7 deg, the coupling between the pitching mode and wing 1st symmetric bending mode is even stronger, with a flutter speed of 16.3 m/s and flutter frequency of 2.1 Hz.

Figure 11 gives a comparison of the 7th order frequency and damping for different swept angles. The results show that the speed at which the pitching mode and 1st symmetric bending mode frequencies start to couple decreases as the swept angle increases. Moreover, the 7th over damping begins to change at this speed.

In conclusion, for swept wing configuration with defined size, BFF is susceptible to occur when the swept angle is increased to an appropriate value. With the increase of the swept angle, the flutter velocity decreases gradually, and the coupling between the pitching mode and the 1st symmetric bending mode becomes stronger.

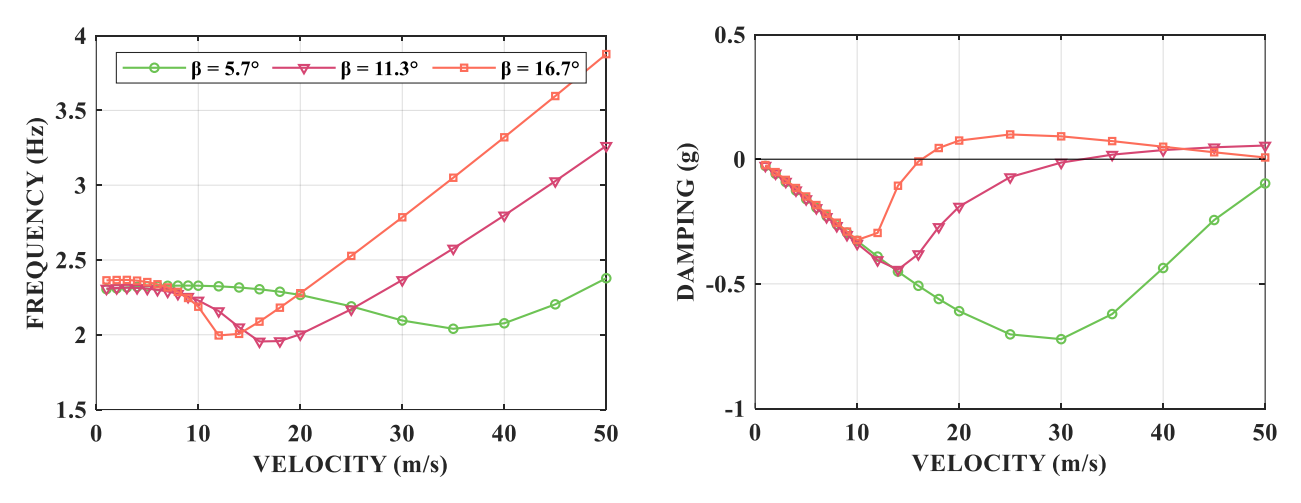


Figure 11 – A comparison of the 7th order frequency and damping for different swept angles.

3.2.3 The influence of payload

The payload magnitude can have a significant effect on the inertial parameters of a flight model, which in turn affects the flutter characteristics of the model. The flutter characteristics of the models with swept angles of 5.7 deg and 11.3 deg at different payload, which is still located 0.15m behind the cross-beam of the fuselage, are presented in Tables 4 and 5, respectively.

Table 4 – The flutter characteristics under different payload (the swept angle is 11.3 deg).

Payload / kg	Flutter speed / m/s	Flutter frequency / Hz
0	/	/
0.1	/	/
0.2	40.1	2.89
0.3	34.1	2.58
0.4	32.1	2.45

Table 5 – The flutter characteristics under different payload (the swept angle is 16.7 deg).

Payload / kg	Flutter speed / m/s	Flutter frequency / Hz
0	17.6	2.25
0.1	17.2	2.21
0.2	16.9	2.17
0.3	16.6	2.14
0.4	16.3	2.10

From the results of the two swept angles, the flutter speed is decreasing as the mass of payload increasing. Because the natural frequency of the model is reduced with the increasing of payload, the pitching mode and 1st symmetric bending mode can start to couple at lower frequency and velocity, leading to a reduction in the critical flutter speed. Consequently, the flutter frequency is also decreasing as the mass of payload increasing.

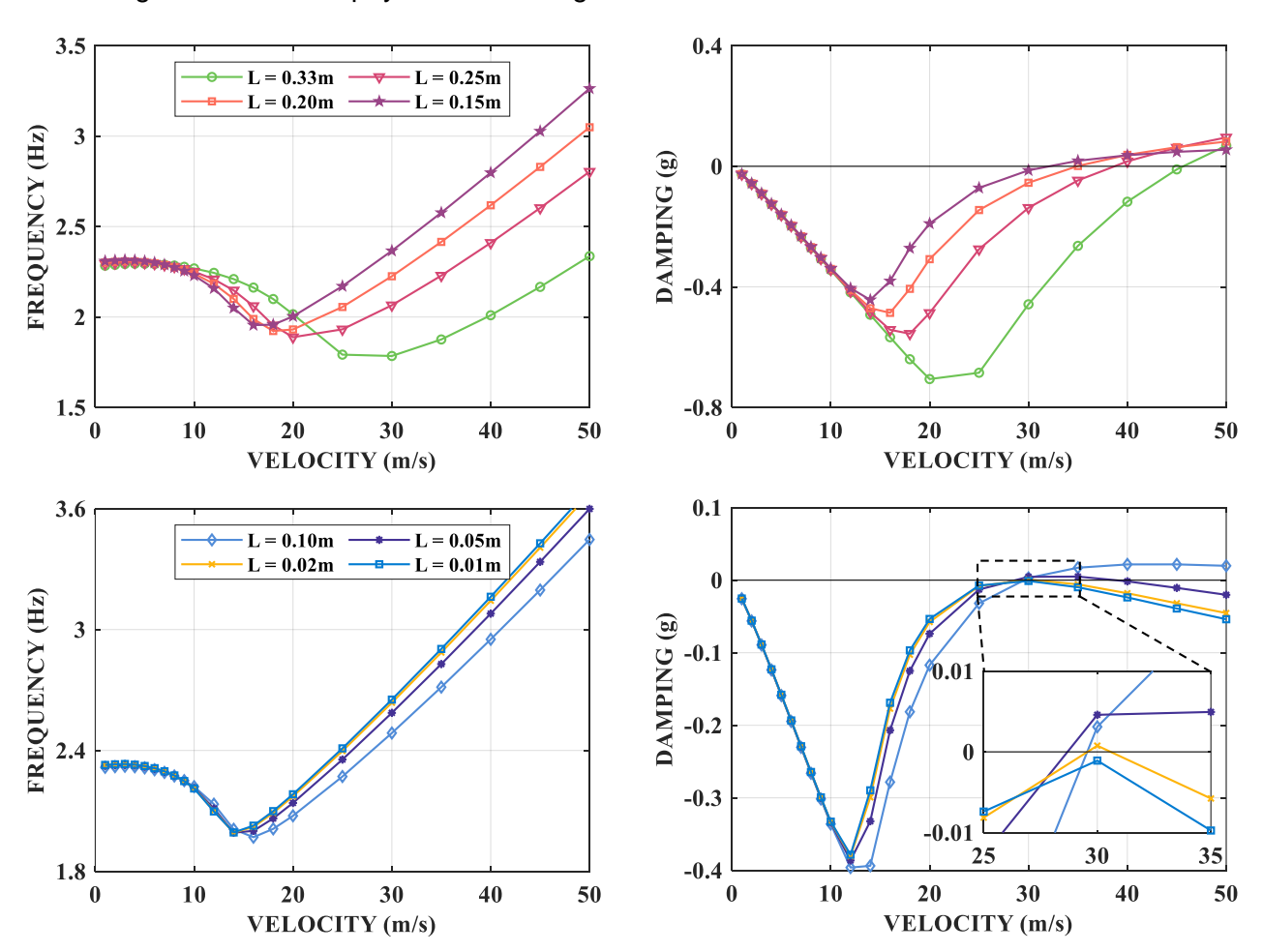


Figure 12 – A Comparison of V-F and V-G diagrams of the wing 1st symmetric bending mode under different location of the payload when the swept angle is 11.3 deg.

Table 6 – The flutter characteristics Corresponding to Figure 12.

ramera a manara anamana a arraap arramig ta migana nen				
Distance of the payload is behind the cross-beam / mm	Flutter speed / m/s	Flutter frequency / Hz		
0.33	45.6	2.19		
0.25	38.7	2.36		
0.20	34.9	2.41		

0.15	32.1	2.45
0.10	29.5	2.46
0.05	28.6	2.52
0.02	29.5	2.61
0.01	/	/

In addition, the location of the payload also has a significant effect on the inertial parameters of a flight model, which in turn affects the flutter characteristics of the model. Based on 0.4kg payload, Figure 12 gives a comparison of V-F and V-G diagrams of the wing 1st symmetric bending mode under different location of the payload when the swept angle is 11.3 deg, and Table 6 lists the corresponding flutter characteristics under different location of the payload. From the results, the flutter speed decreases firstly when the payload is moved from the tail to the center of the fuselage. Interestingly, when moving forward to a certain position, the flutter speed increases slightly until it finally disappears. But for flutter frequency, it monotonically keeps increasing.

With the same mass of payload, Figure 13 gives a comparison of V-F and V-G diagrams of the wing 1st symmetric bending mode under different location of the payload when the swept angle is 16.7 deg, and Table 6 lists the corresponding flutter characteristics. Where 'L=-0.1m' means that the payload is located before the cross-beam of the fuselage. The results obtained are somewhat different from those obtained previously. The flutter speed also decreases and then increases slightly with the forward movement of the payload. The difference is that the flutter frequency has become first decreases and then increases, i.e., the flutter frequency does not monotonically increase. The possible reason for this situation is that the gravity center of the model is backward when the swept

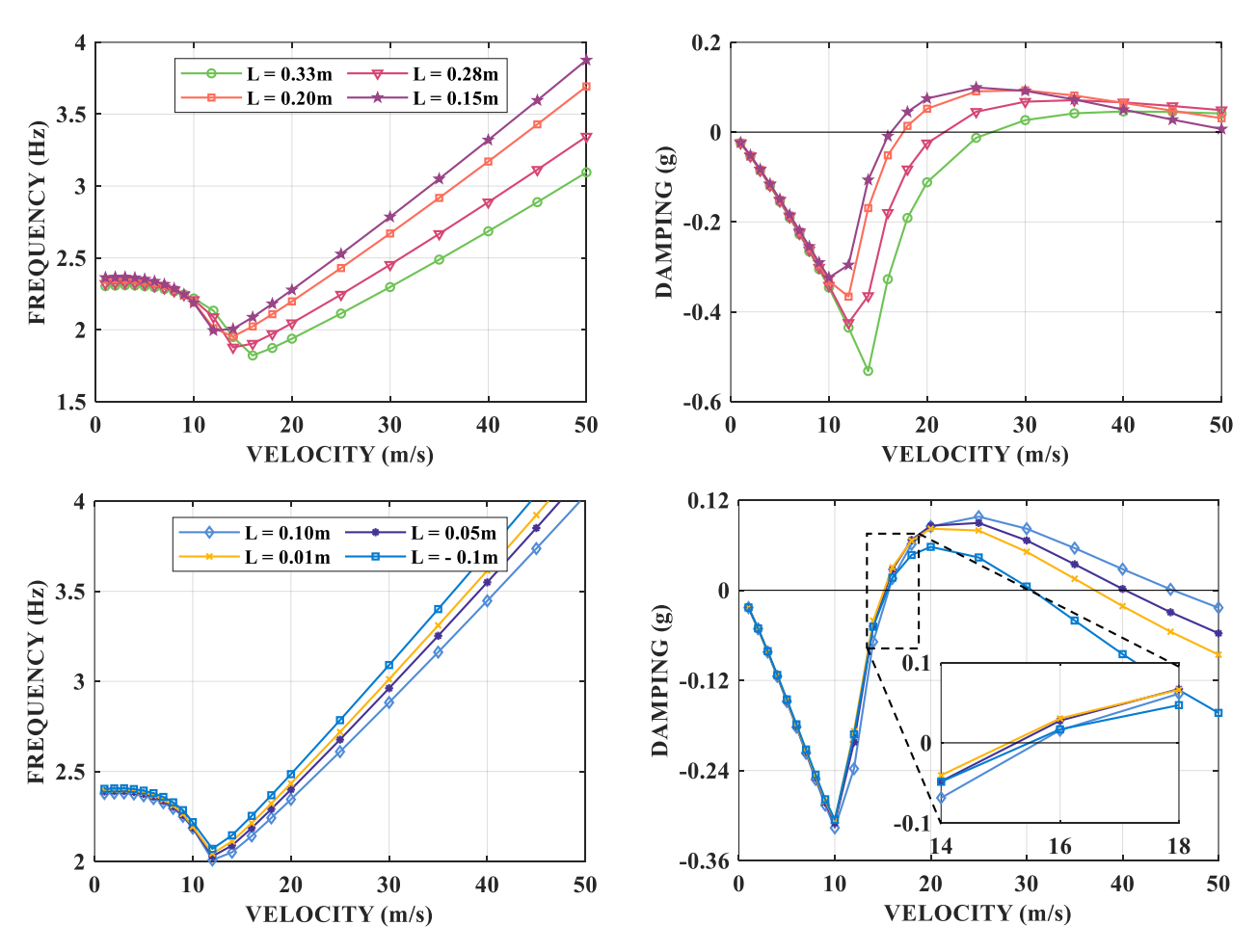


Figure 13 – A Comparison of V-F and V-G diagrams of the wing 1st symmetric bending mode under different location of the payload when the swept angle is 16.7 deg.

Table 7 – The flutter characteristics Corresponding to Figure 13.	Table 7 –	The flutter	characteristics	Corresponding	to Figure 13.
---	-----------	-------------	-----------------	---------------	---------------

Distance of the payload is behind the cross-beam / mm	Flutter speed / m/s	Flutter frequency / Hz
0.33	26.6	2.172
0.25	21.7	2.114
0.20	17.5	2.087
0.15	16.3	2.102
0.10	15.6	2.124
0.05	15.2	2.147
0.01	15.1	2.156
-0.1	15.4	2.221

angle is too large, and the monotonically increase of the flutter frequency needs to satisfy the condition that the location of gravity center is forward, which is just satisfied in the case of the swept angle of 11.3 deg. Moreover, the payload position corresponding to the flutter speed reversal at the swept angle of 16.7 deg is also located before the position that the swept angle of 11.3 deg corresponding to, indirectly proving the correctness of the above potential reason.

So far, we have completed all theoretical analyses of the designed BFF model, including the influence of aerodynamic layout, the mass and location of the payload. The following section will introduce the completion of the vehicle based on the theoretical calculations.

4. Model fabrication and test

4.1 GVT

The designed flutter speed could be achieved according to a previous performance evaluation. One vehicle with a swept angle of 11.3 deg was built for GVT and later taxiing and test flight. The fabricated vehicle with airborne instruments is shown in Figure 14. The whole fuselage is 3D printed in abs. The wing main beams and cross-beam of the fuselage are 7075 aluminum alloy, while epp material is used for the wing body. The gross takeoff weight is 3.5 kg.

The GVT setup is shown as Figure 15. The vehicle is suspended by a soft enough bungee cord and the suspension mode is well separated from the fundamental elastic mode.

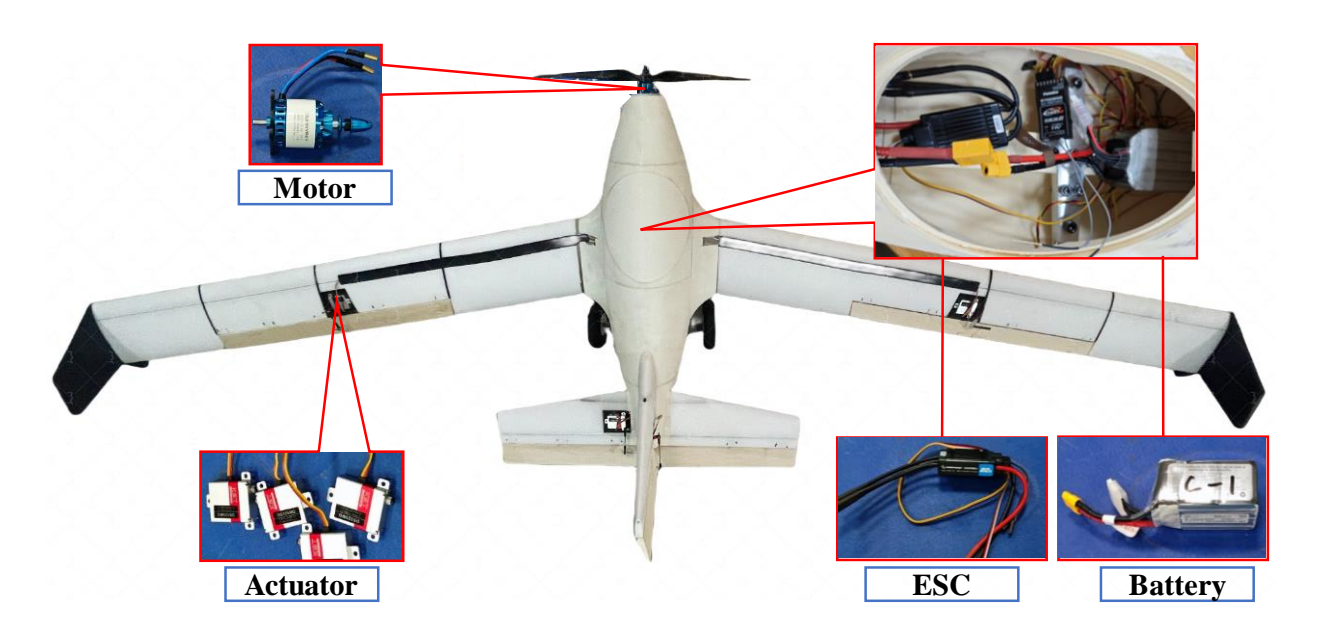


Figure 14 – BFF vehicle.

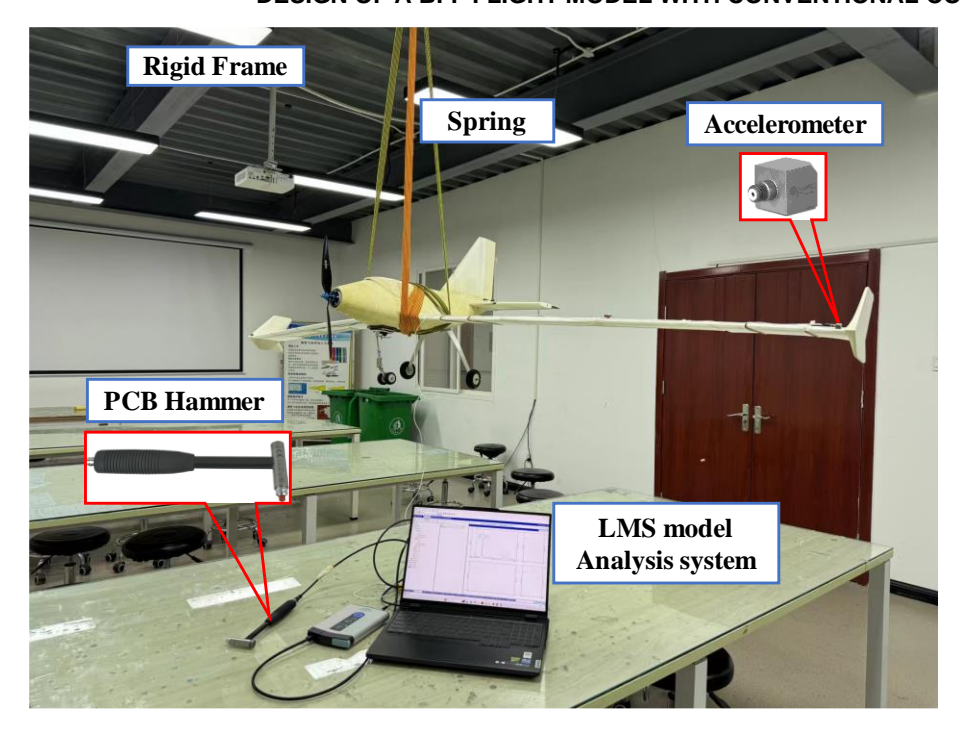
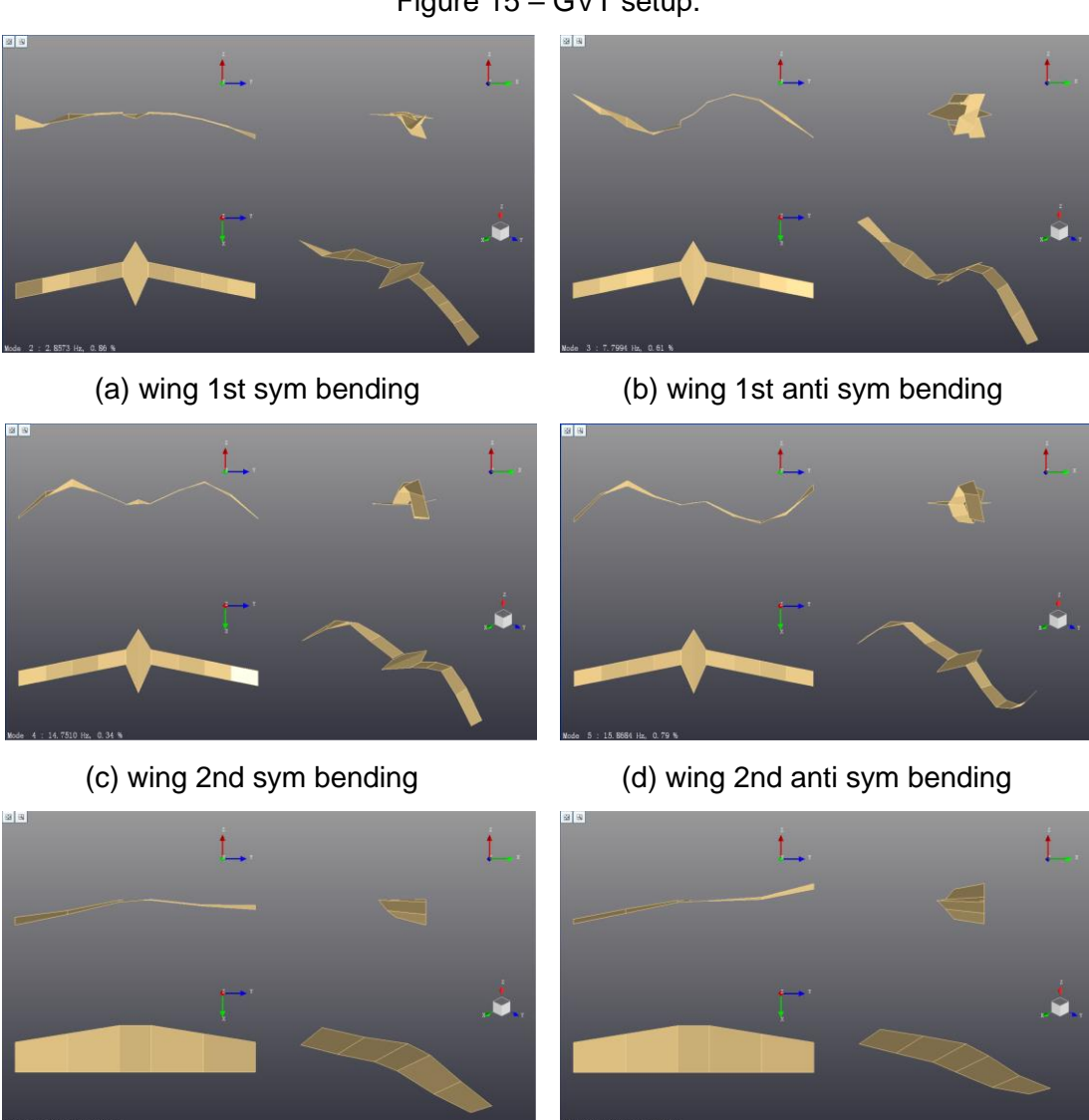


Figure 15 – GVT setup.



(e) H-tail 1st sym bending

(f) H-tail 1st anti sym bending

Figure 16 – Test mode shapes.

Table 8 Modal frequency comparison

Modes	Test results / Hz	Theoretical / Hz	Theoretical updated / Hz	Relative error
1st sym wing bending	2.857	2.787	2.748	-3.82%
1st anti sym wing bending	7.799	10.971	10.061	29.00%
2nd sym wing bending	14.751	16.633	16.944	14.87%
2nd anti sym wing bending	15.868	17.683	17.238	8.63%
1st sym H-tail bending	23.699	NA	NA	NA
1st anti sym H-tail bending	41.014	NA	NA	NA

The GVT results are shown in Table 8. The first six elastic mode shapes are shown in Figure 16.

By tuning the Young's modulus alone, the FEM model is updated according to the test results and also shown in Table 8. Observably, the natural frequency of the updated wing 1st symmetric bending mode correlates well with the test value. As the fuselage and the empennage are modelled as rigid element, no comparisons were available for related modes. At the same time, it is noted that the wing 1st antisymmetric bending mode frequency is still much higher than the test value, which may be a limitation of modifying only the elastic modulus of the wing main beam.

Flutter analysis is conducted based on the updated model. To 'produce' BFF in the vehicle, 0.4kg payload is still utilized, which is located 0.15m behind the cross-beam of the fuselage. Finally, the flutter speed is 30.4 m/s and the flutter frequency is 2.45 Hz, which is dominated by the coupling between the rigid body pitch and the wing 1st symmetric bending modes, as shown in Figure 17.

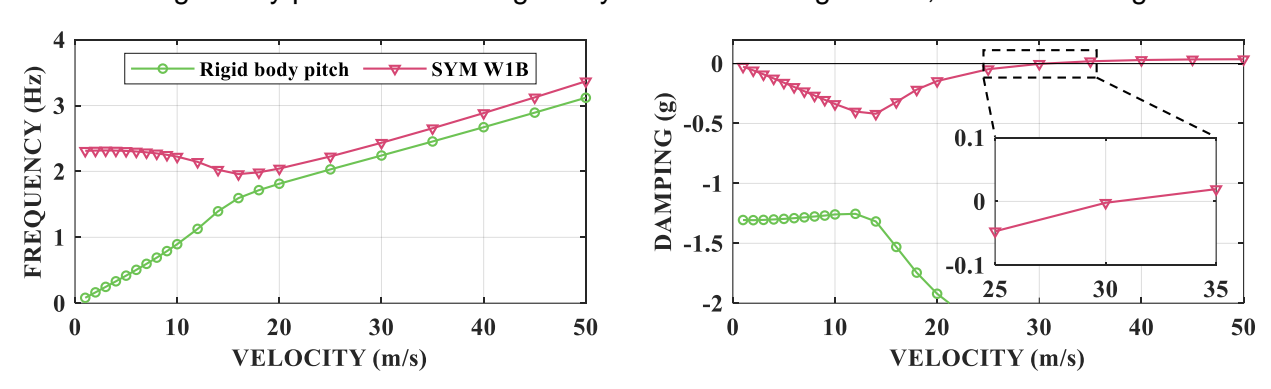


Figure 17 – The V-F and V-G diagrams after model updating.

4.2 Taxiing and preliminary test flight

After GVT, the vehicle was delivered for ground taxiing. The taxiing and preliminary flight for the BFF vehicle were conducted as shown in Figure 18, which show a good to go for future flight flutter test.



Figure 18 – Taxiing (a) and airborne (b) of the BFF vehicle.

5. Conclusions

Similar to the BWB configuration, it was demonstrated that there may also exist BFF instability for conventional configuration aircraft with very short fuselage. The influence of aerodynamic layout, the mass and location of the payload on the flutter characteristics were analyzed in detail using FEM. A BFF vehicle of such category is designed and still under flight testing. It is expected to get encouraging results in the near future.

6. Contact Author Email Address

Xinhai Tian: txh@mail.nwpu.edu.cn

Yingsong Gu: guyingsong@nwpu.edu.cn

7. Copyright Statement

The authors confirm that they, and/or their company or organization, hold copyright on all of the original material included in this paper. The authors also confirm that they have obtained permission, from the copyright holder of any third party material included in this paper, to publish it as part of their paper. The authors confirm that they give permission, or have obtained permission from the copyright holder of this paper, for the publication and distribution of this paper as part of the ICAS proceedings or as individual off-prints from the proceedings.

References

- [1] Banerjee J.R. Flutter characteristics of high aspect ratio tailless aircraft. *Journal of Aircraft*, Vol. 21, No. 9, pp 733-735, 1984.
- [2] Banerjee J.R. Flutter modes of high aspect ratio tailless aircraft. *Journal of Aircraft*, Vol. 25, No. 5, pp 473-476, 1988.
- [3] Niblett LL.T. The fundamentals of body-freedom flutter. *The Aeronautical Journal*, Vol. 90, No. 899, pp 373-377, 1986.
- [4] Bansal P. and Pitt D.M. Effects of variations in structural properties of a generic wing on flutter prediction. 53rd AIAA/ASME/ASCE/AHS/ASC Structures, Structural Dynamics, and Materials Conference, AIAA Paper, 2012-1795, 2012.
- [5] Phillip W.R, Yuan Y, Robert A.H, et al. Effect of inertial and constitutive properties on body-freedom flutter for flying wings. Journal of Aircraft, Vol. 53, No. 5, pp 756-767, 2016.
- [6] Liu J.H, Gu Y.S, Yang Z.C. Influence of support stiffness on natural mode and body freedom flutter characteristics of a flying wing model. Journal of Vibration Engineering, Vol. 31, No. 5, pp 727-733, 2018.
- [7] Shi P.T, Liu J.H, Gu Y.S, et al. Full-span flying wing wind tunnel test: a body freedom flutter study. Fluids, Vol. 5, No. 1, 2020.
- [8] Shi P.T, Liu F, Gu Y.S, et al. The development of a flight test platform to study the body freedom flutter of BWB flying wings. Aerospace, Vol. 8, No. 12, 2021.
- [9] Ang E.H.W, Leo D.J, Tan J.K, et al. Wind tunnel experiments of bending-torsion and body-freedom flutter on flying wing unmanned aerial vehicles. Aerospace Science and Technology, Vol. 144, 108798, 2024.
- [10]Love M.H, Zink P.S, Wieselmann P.A, et al. Body freedom flutter of high aspect ratio flying wings. AIAA-2005-1947, 2012.